International Journal of Refrigeration 152 (2023) 387–399

Contents lists available at ScienceDirect

International Journal of Refrigeration

journal homepage: www.elsevier.com/locate/ijrefrig

Alternative CO_2-based blends for transcritical refrigeration systems

Mélanges alternatifs à base de CO_2 pour les systèmes frigorifiques transcritiques

D. Sánchez [a,*], F. Vidan-Falomir [a], R. Larrondo-Sancho [a], R. Llopis [a], R. Cabello [a]

[a] *Jaume I University, Dep. of Mechanical Engineering and Construction, Campus de Riu Sec s/n E-12071, Castellón, Spain*

ARTICLE INFO

Keywords:
CO_2
COP
Binary mixture
R32
R1270
R1234yf
Mots clés:
CO_2
COP
Mélange binaire
R-32
R1270
R1234yf

ABSTRACT

The extensive use of CO_2 in commercial refrigeration system has grown in the last two decade thanks to the development of new components and configurations that allows working in transcritical conditions efficiently. However, using these arrangements increases the cost and complexity of the refrigerating plant, making it challenging to implement them in medium or low-capacity systems. As an alternative, CO_2-based binary mixtures report attractive improvements that allow for enhancing the COP of the system by minimising its complexity and maintaining the safety and environmental conditions of CO_2. This manuscript analyses five binary mixtures of CO_2 with the refrigerants R32, R152a, R1234yf, R1234ze(E) and R1270, determining the optimal mixture composition for maximising the COP of a CO_2 transcritical refrigeration plant in a wide range of environmental temperatures (0 to 40°C). Fixing the operating conditions for a medium-temperature application, the binary mixtures of C_{O2}/R32 (81/19% in mass) and CO_2/R1270 (92.5/7.5% in mass) reported the best COP enhancements results with increments up to +21.4% and +8.7%, respectively, at high environmental temperatures.

1. Introduction

Thanks to its environmental compatibility, non-flammability, high availability and relatively good transport and heat transfer properties, carbon dioxide (CO_2 or R744) has been established as a powerful alternative to current anthropogenic refrigerants in commercial refrigeration. Taking into account the impact of this sector in terms of greenhouse-gas emissions (7.8% in 2014 (Morlet et al., 2017)), the solution of using natural refrigerants has raised significantly focus on solving the main issues historically related to those: flammability for hydrocarbons, toxicity for ammonia and low performance for CO_2 at warm environmental temperatures (Lorentzen, 1995). For CO_2, the low performance is related to its low critical temperature (~31°C), which forces the refrigeration cycle to work in transcritical conditions during the heat rejection process. Despite the excellent hat transfer process under these conditions, transcritical cycles introduce high irreversibilities during the compression and expansion process penalising the COP of the cycle (Kim et al., 2004). As a result, the classic vapour compression cycle adopted for artificial cold production is modified, and different arrangements are introduced to enhance the cycle's performance and reduce the heat rejection pressure. Most use the suction-to-liquid heat exchanger (IHX) to increase the specific cooling capacity (Torrella et al., 2011, Sánchez et al., 2014), but others introduce more complex arrangements with different benefits in subcooling and working pressures. Some examples are the flash-gas by-pass valve (Elbel and Hrnjak, 2004, Cabello et al., 2012), the parallel compressor (Chesi et al., 2014), ejectors (Haida et al., 2016, Singh et al., 2020), or the adoption of active subcooling systems at the exit of the gas-cooler (Bellos and Tzivanidis, 2019, Sánchez et al., 2020, Aranguren et al., 2021). However, excepting the IHX, these methods increase the cost of the plant and its complexity, so most of them are only targeted to large-capacity systems as centralized systems.

The search for low-cost, effective methods to enhance the performance of CO_2 cycles leads to the use of CO_2-based blends based on the idea of doping pure C_{O2} with small quantities of other fluids to modify the thermophysical properties of CO_2. This concept was presented by Kim & Kim (Kim and Kim, 2002) in 2002 to enhance the performance of an auto-cascade, and by Di Nicola et al. (Di Nicola et al., 2005) in 2005 to extend the operation of CO_2 below its triple point. Later, blends were orientated to increase the critical temperature and reduce the critical pressure, boosting the subcritical operation range of pure CO_2 (Cox

* Corresponding author.
E-mail address: sanchezd@uji.es (D. Sánchez).

https://doi.org/10.1016/j.ijrefrig.2023.03.021
Received 29 November 2022; Received in revised form 5 March 2023; Accepted 15 March 2023
Available online 21 March 2023

Nomenclature

COP	Coefficient Of Performance
FIP	Fuel Inertization Point
GWP	Global Warming Potential
h	specific enthalpy ($kJ \cdot kg^{-1}$)
HC	HydroCarbon
HFC	HydroFluoroCarbon
HFO	HydroFluoroOlefin
IHX	Internal Heat Exchanger
LFL	Lower Flammability Limit (%)
LMTD	Logarithmic Mean Temperature Difference (K)
$\dot{m}$	mass flow rate ($kg \cdot s^{-1}$)
N	compressor rotation speed (rpm)
NBP	Normal Boiling Point (°C)
ODP	Ozone Depletion Potential
P	pressure (bar)
$\dot{Q}$	heat transfer rate (W)
SH	superheating (K)
T	temperature (°C)
UFL	Upper Flammability Level (%)
v	specific volume ($m^3 \cdot kg^{-1}$)
VCC	Volumetric Cooling Capacity ($kJ \cdot m^{-3}$)
$\dot{V}$	compressor cubic capacity ($m^3 \cdot h^{-1}$)
$\dot{W}$	power input (W)
x	vapour quality
X	refrigerant mass fraction (%)

Greek symbols

Δ	variation (increment or decrement)
ε	maximum deviation (%)
η	efficiency (%)

Subscripts

air	air
blend	it refers to the mixture
bp	back-pressure
cal	calculated
CO_2	it refers to CO_2
crit	critical point
dis	discharge
env	environmental
ev	evaporator
G	geometric / global
gas	it refers to the additional fluid in the mixture
gc	gas-cooler
hp	high-pressure side
i	inlet
in	initial
iso	isoentropic
k	condenser
m	it refers to molar
max	maximum
min	minimum
mix	it refers to the mixture
opt	optimum
o	out
suc	suction port
V	volumetric
w	it refers to mass

et al., 2008). Moreover, the glide resulting from the zeotropic mixture was suggested for a better matching between the refrigerant and the secondary fluid, reducing the irreversibility during the heat exchange process (Kim et al., 2008).

In the last decade, different authors have theoretical and experimentally analysed various CO_2-based blends as refrigerants in vapour compression systems. Thus, Niu & Zhang (Niu and Zhang, 2007) demonstrated experimentally the convenience of using CO_2/R290 (71/29%m) instead of R13 in a cascade system for temperatures below -58°C. Kim et al. (Kim et al., 2008) proved experimentally that the mixture of CO_2/R290 (75/25%w) performs +12.8% better than pure CO_2 in an air conditioning system with a decrement in the cooling capacity of -22.7%. Sarkar & Bhattacharyya (Sarkar and Bhattacharyya, 2009) computed the use of mixtures CO_2/R600 (50/50%w) and CO_2/R600a (50/50%w) instead of CO_2 in a high-temperature heat pump. The results revealed drops in COP of-9.5% and -1.8%, respectively, with lower working pressures. Dai et al. (Dai et al., 2015) theoretically analysed ten different CO_2-based blends with R41, R32, R161, R134a, R152a, R290, R1270, RE170, R1234yf and R1234ze(E), resulting in the mixtures CO_2/R41 (40/60%w) and CO_2/R32 (80/20%w) as the most relevant in a heat pump water heater, with COP increments of 4.0% and 4.5%, respectively. Bouteiller et al. (Bouteiller et al., 2016, Bouteiller et al., 2017) tested in conditions of a domestic water heater and central heating, the blends of CO_2/R290 (85/15%m) and CO_2/R1234yf (94.5/5.5%m), resulting in a slight reduction of the performance at the first operating conditions, and a slight increase in the second case. Wang et al. (Wang et al., 2017) also computed a heat pump water heater and a refrigerated cabinet with the blend CO_2/R41 (50/50%w), obtaining a COP and cooling capacity enhancement of 20.5% and 25.7%, respectively. Yu et al. (Yu et al., 2018, Yu et al., 2019) tested mobile air conditioning with CO_2/R290 and CO_2/R41, obtaining COP increments up to 22.1% and 25.7%, respectively. Ju et al. (Ju et al., 2018) compared the operating conditions of a heat pump water heater with the blend of CO_2/R290 (88/12%w) and the HCFC R22 experimentally, resulting in a COP and heating capacity improvement of 11.0% and 17.5%, respectively. Sun et al. (Sun et al., 2019), also for a heat pump water heater and cooling, demonstrate experimentally that the binary mixture of CO_2/R32 allows increasing the COP of the cycle either for cooling or heating, but with a reduction in the cooling capacity. Sánchez et al. (Sánchez et al., 2023) optimized a CO_2 vertical beverage cooler energetically using the binary mixtures of CO_2/R1270 (92.5/7.5%w) and CO_2/R32 (78/22%w). The results provided energy savings of up to 15.7% and 17.2%, respectively, at class III climate conditions (25°C, 60%). Xie et al. (Xie et al., 2021) compared the blends of CO_2/R152a (82.5/17.5%w) and CO_2/R161 (85/15%w) with pure CO_2 in a transcritical refrigeration cycle theoretically, resulting in COP improvements up to 30.1% and 32.5%, respectively. Finally, Vaccaro et al. (Vaccaro et al., 2022) compared, from a computational model, four typical arrangements of CO_2 cycles using different binary blends of CO_2. The mixtures of CO_2/R1234yf and CO_2/R290 resulted as the best alternative to pure CO_2, with COP increments up to 12.8% and 7.9%, respectively.

Taking into account the results provided by other authors, the use of CO_2-based blends is an attractive solution geared towards enhancing the performance of CO_2 transcritical cycles with an apparent easy implementation. However, no deep analysis has been found in the literature about optimising the CO_2 mixtures considering restrictions about flammability or compressor size. Therefore, the present work investigates five CO_2 binary mixtures as alternatives to pure CO_2 in commercial refrigeration, considering the restrictions of non-flammability and GWP below 150. The mixtures with R32, R152a, R1234yf, R1234ze(E) and R1270 are analysed with a computational model in a wide range of environmental temperatures (from 0 to 40°C), using as a cooling load a medium-temperature cabinet for fresh-food preservation.

2. Fluid selection

2.1. Adopted criteria

The main criterion used to determine the fluids that define the binary mixtures is the high availability of the fluids in the marked according to the current environmental regulations. Thus, all the fluids with ODP higher than 0 and a GWP higher than 800 have not been considered since they can be limited in incoming new regulations. Therefore, this study selected five fluids: R32 and R152a as HFCs, R1234yf and R1234ze(E) as HFOs, and R1270 as HC. The main properties of these fluids are summarized in Table 1.

The thermophysical identified in Table 1 correspond to molar mass, normal boiling point (NBP), critical pressure (Pcrit), and critical temperature (Tcrit). The safety classification is determined with the ASHRAE Standard 34 (ASHRAE 2019), and the low and upper flammability limits (LFL, UPL) are taken from Calm (Calm, 1999) and the manufacturer Honeywell (Honeywell 2018, Honeywell 2008). Finally, the GWP is considered with a horizon of 100 years.

The second criterion adopted for binary mixtures corresponds to the non-flammability condition since those blends could be used as drop-ins in an existing CO_2 transcritical plant. Moreover, the mixture GWP must be under the limits proposed by the EU regulation n° 514/2014. Therefore, the third criterion corresponds to the maximum value of the GWP, which should be lower than 150 in any case.

Focusing on the restriction of non-flammability, all fluids selected are flammable, with a flammability range defined by the upper and lower flammability limits. This flammability range can be reduced by adding an inert gas such as pure C_{O2} until both limits coincide at a point called Fuel Inertization Point (FIP). The FIP defines the maximum concentration of flammable gas in the dry air - gas - CO_2 mixture that never generates a flammable mixture regardless of the amount of air added or removed from the mixture (Kondo et al., 2006). Therefore, it fixes the maximum concentration of the flammable gas that can be added to C_{O2}, maintaining non-flammable theoretical conditions. The work presented by Kondo et al. [38] defines the mathematical model to determine the UFL and the LFL depending on the flammable gas used and the CO_2 added. The results are gathered in Table 2, where the GWP is determined by Eq. (1) with the mass fraction of both fluids (X), ensuring the third criterion (Eq. 2).

$$GWP_{mix} = X_{w\ CO2} GWP_{CO2} + X_{w\ gas} GWP_{gas} \quad (1)$$

$$\frac{150 - X_{w\ CO2} GWP_{CO2}}{GWP_{gas}} > X_{w\ gas} \quad (2)$$

2.2. Thermophysical properties of binary mixtures

To compare the proposed blends, the thermophysical properties of the critical point (temperature and pressure), latent heat of evaporation, total glide, volumetric cooling capacity (VCC) and specific compression work are presented at different percentages of the additional fluid. Figs. 1 to 3 present these properties indicating the flammability limit for each mixture according to Table 2. Properties below this limit are depicted in solid lines, while properties above the limit are shown in dash lines. The software used to evaluate thermophysical properties was RefProp® v.10.0 (Lemmon et al., 2018), which estimates the properties of mixtures by using mixing rules with a series of interaction parameters to the Helmholtz Energy adjusted from experimental or theoretical simulations data (Bell and Lemmon, 2016). For CO_2 blends with R32, R152a and R1270, these parameters are fitted from empirical data, while for hydrofluoroolefins R1234yf and R1234ze(E), the parameters are estimated using the simulation data from Raabe (Raabe, 2013). The results obtained from this last were corroborated later by Bell et al. (Bell et al., 2021) with different experimental data resulting in a good concordance adequate for engineering designs. Therefore, the results obtained from RefProp® are suitable for this study.

Adding fluid to pure CO_2 modifies its critical point by increasing the temperature (Fig. 1A) and the critical pressure (Fig. 1B). The increment of the critical temperature extends the subcritical operation of the plant, while the parabolic evolution of the critical pressure reduces the pressure levels in the refrigerating plant, easing the component's design and requirements.

According to Fig. 2, doping CO_2 with other fluid maximises the latent evaporation heat in all cases being higher for the hydrocarbon R1270, followed by the HFCs R152 and R32, and the HFOs R1234ze(E) and R1234yf. The rise of the latent heat allows reducing the refrigerant mass flow rate for a demanding cooling capacity, which also reduces the compressor work.

Similarly to evaporation latent heat, the total glide rises with a maximum that depends on the NBP difference between the fluids. According to Mulroy et al. (Mulroy et al., 1994), the higher this difference is, the higher the total glide will be. Hence, using data from Table 1, there is a concordance between the maximum of the total glide and the NBP temperature difference. Notwithstanding, considering the flammable limitation of Table 2, mixtures of R1270 and R32 will provide lower values of total glide, while the values for R152a and HFOS R1234yf and R1234ze(E) will be high.

The volumetric cooling capacity (VCC) (Fig. 3A) is defined as the quotient between the latent evaporation heat and the specific volume at the vapour-saturated conditions. Combining CO_2 with other refrigerants drastically reduces this parameter due to the specific volume increment, which offsets the latent heat improvement. Consequently, the cubic compressor capacity for CO_2-based blends must be higher than pure-CO_2

Table 2
Limit of composition for non-flammable conditions.

Mixture	FIP [a]	% C_{O2} (in mass)	% Flammable Gas (in mass)	GWP_{100}
CO_2 / R32	56.1%	80.7%	19.3% [b]	149.6
CO_2 / R152a	79.5%	79.5%	20.5%	26.7
CO_2 / R1234yf	44.6%	44.6%	55.4%	2.7
CO_2 / R1234ze(E)	36.6%	36.6%	63.4%	4.8
CO_2 / R1270	92.4%	92.4%	7.6%	1.1

[a] percentage in mass of C_{O2} in the mixture of flammable gas and C_{O2}.
[b] limited by the maximum GWP allowed (150)

Table 1
Main properties of the fluids analysed.

Name	Family	Molar mass (g·mol^{-1})	NBP (°C)	P_{crit} (bar)	T_{crit} (°C)	Safety group	LFL (%)	UFL (%)	GWP_{100}
R744	Inorganic	44.0	-78.4	73.8	31.1	A1	-	-	1 [a]
R32	HFC	52.0	-51.7	57.8	78.1	A2L	13.3	29.3	771 [a]
R152a	HFC	66.0	-24.0	45.2	113.2	A2	4.3	17.4	164 [a]
R1234yf	HFO	114.0	-29.5	33.8	94.7	A2L	6.2	12.3	4 [c]
R1234ze(E)	HFO	114.0	-19.0	36.3	109.4	A2L	7.0	12.0	7 [c]
R1270	HC	42.1	-47.7	46.7	92.4	A3	2.2	11.0	2 [b]

[a] IPCC AR6 (IPCC, 2021)
[b] Hodnebrog *et al.* (Hodnebrog et al., 2018)
[c] IPCC AR5 (Climate Change, 2014)

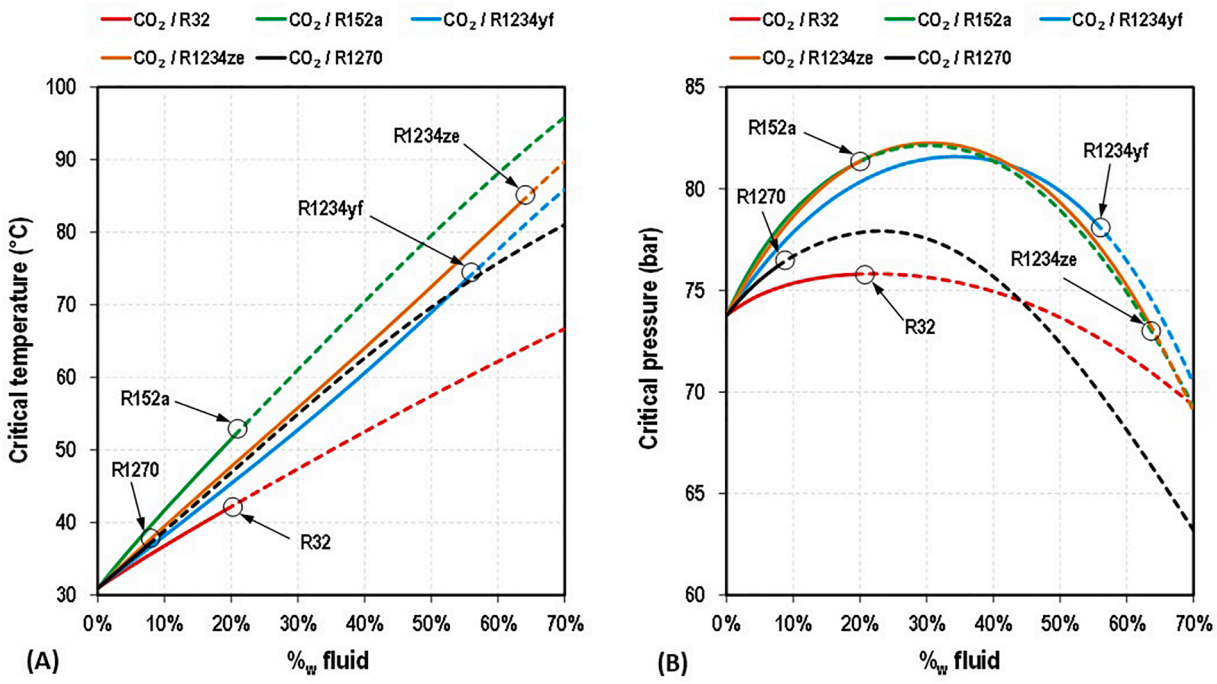

Fig. 1. Critical temperature (A) and pressure (B) vs mass fraction of additional fluid.

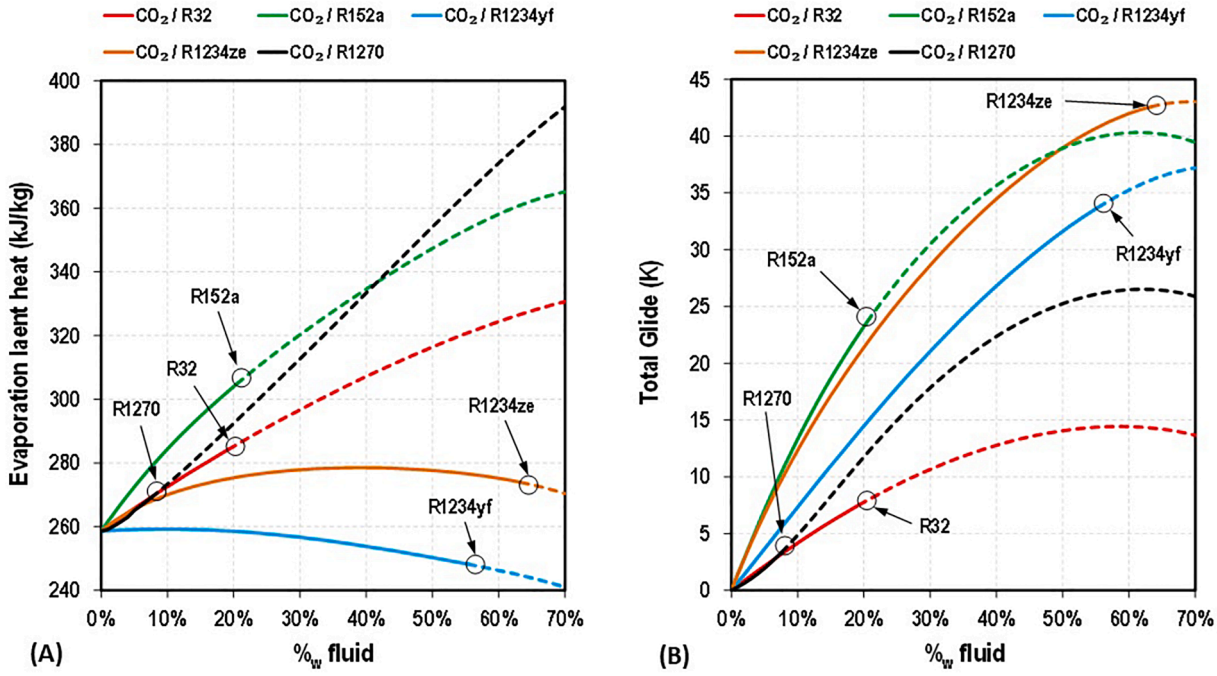

Fig. 2. Evaporation latent heat (A) and total glide (B) vs mass fraction of additional fluid (T_{ev}: -10°C; x_{ev}: 50%).

to obtain the same cooling capacity. This issue could be fixed by increasing the compressor rotation speed or combining several compressors simultaneously in an existing refrigeration plant.

Finally, the specific compressor work is calculated assuming an isentropic compression process and a discharge pressure defined by the heat rejection temperature of 30°C and vapour quality of 50%. The results presented in Fig. 3 right predict that R1234yf and R1234ze(E) always reduce the compressor consumption of the refrigerating plant compared with pure CO_2. However, R152a and R32 increase this value similar to R1270. Considering the flammability limits of Table 2, the maximum increment introduced by the alternative mixtures is 7.0%, while the maximum reduction is up to -23.6%.

3. Computational model

3.1. Cycle configuration

The configuration adopted to analyse the performance of the doped CO_2 binary mixtures is depicted in Fig. 4. It represents the basic arrangement usually adopted in transcritical refrigeration cycles with a

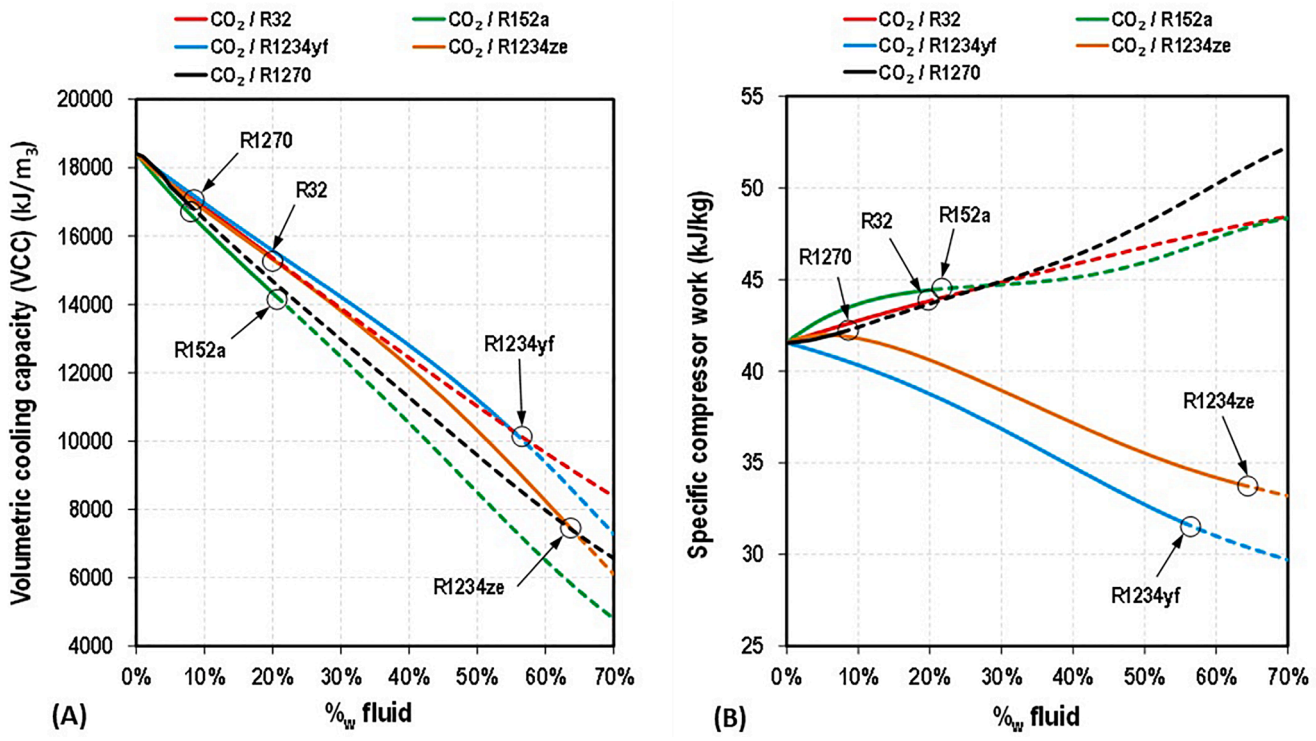

Fig. 3. Volumetric cooling capacity (A) and specific compression work (B) vs mass fraction of additional fluid (T_{ev}: -10°C; x_{ev}: 50%; T_k: 30°C; x_k: 50%).

unique cooling service and two-stage expansion system controlling simultaneously heat rejection pressure and the evaporator's useful superheating.

3.2. Model input data and restrictions

Table 3 summarizes the main variables considered as input data of the computational model. The values of approach temperatures (ΔT_{env}), useful and non-useful superheating degrees (SH_{suc}, SH_{ev}) and pressure drop in the back pressure valve working in subcritical conditions (ΔP_{bp}) were taken from the work published by Catalán-Gil et al. (Catalán-Gil et al., 2018). The cooling capacity ($\dot{Q}_{ev}$) was assumed constant with a value of 5KW, while the environmental temperature (T_{env}) was varied in a wide range from 0 to 40°C considering different environmental cases from cold to hot climates.

Due to the zeotropic behaviour of CO_2-based mixtures, the evaporator has been modelled with the air temperature at the inlet and outlet of the evaporator ($T_{air\ i}$, $T_{air\ o}$) and the logarithmic mean temperature (LMTD). The values of these parameters correspond to a medium-temperature cabinet for fresh product preservation analysed by

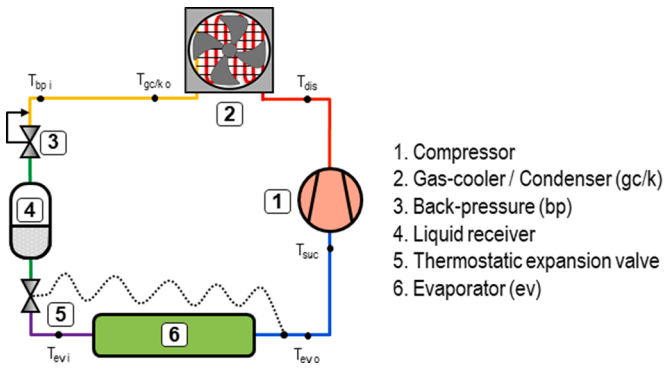

Fig. 4. CO_2 base cycle with two-stage expansion system.

Table 3
Input data to the computation model.

Variable	Description	Value
T_{env}	Environmental temperature	0 to 40°C
ΔT_{env}	Approach temperature in the condenser/gas-cooler	5 / 2K
ΔP_{bp}	Back pressure's pressure drop in subcritical conditions	2 bar
N	Compressor rotation speed	1450 rpm
SH_{suc}	Non-useful superheating	4K
SH_{ev}	Useful superheating	5K
$\dot{Q}_{ev}$	Cooling capacity	5000 W
$T_{air\ i}$	Air inlet temperature (evaporator)	2°C
$T_{air\ o}$	Air outlet temperature (evaporator)	-1°C
LMTD	Logarithmic mean temperature	7K

authors in (Sánchez et al., 2018).

The compressor model used in this work corresponds to a DORIN semi-hermetic compressor model CD300H adjusted from the experimental data published by Catalán-Gil et al. Catalán-Gil et al., 2020) with pure CO_2 by using the polynomial expressions Eq. (3) and ((4) as a function of the discharge and suction pressure (P_{ev} and P_{dis} respectively), and the temperature at the suction port (Tsuc). Table 4 gathers the empirical coefficients of these equations with the maximum deviation (εmax). Since no studies or models about semi-hermetic compressors have been found with the analysed mixtures, we assume the same model for all mixtures.

$$\eta_V = a_0 + a_1 P_{ev} + a_2 P_{dis} + a_3 T_{suc} \quad (3)$$

Table 4
Experimental coefficients for the C_{O2} semi-hermetic compressor.

Coefficient	η_V	η_G
a_0	0.1312788140	0.5934191583
a_1	0.0249667938	-0.0044745055
a_2	-0.0030932686	0.0000441574
a_3	-0.0193683038	0.0038783058
ε_{max}	*0.94%*	*2.21%*

$$\eta_G = a_0 + a_1 P_{ev} + a_2 P_{dis} + a_3 T_{suc} \quad (4)$$

To perform a realistic analysis, the computational model limits the heat rejection pressure to 120 bar, with a minimal pressure of condensation calculated with the ambient temperature. Furthermore, the compression ratio has a minimum of 1.5 to ensure the proper operation of the compressor. Finally, a minimum pressure difference of 2 bar was adopted in the expansion devices, including subcritical conditions. Whatever the needs, the model assumes no pressure drop inside the pipelines and heat exchangers.

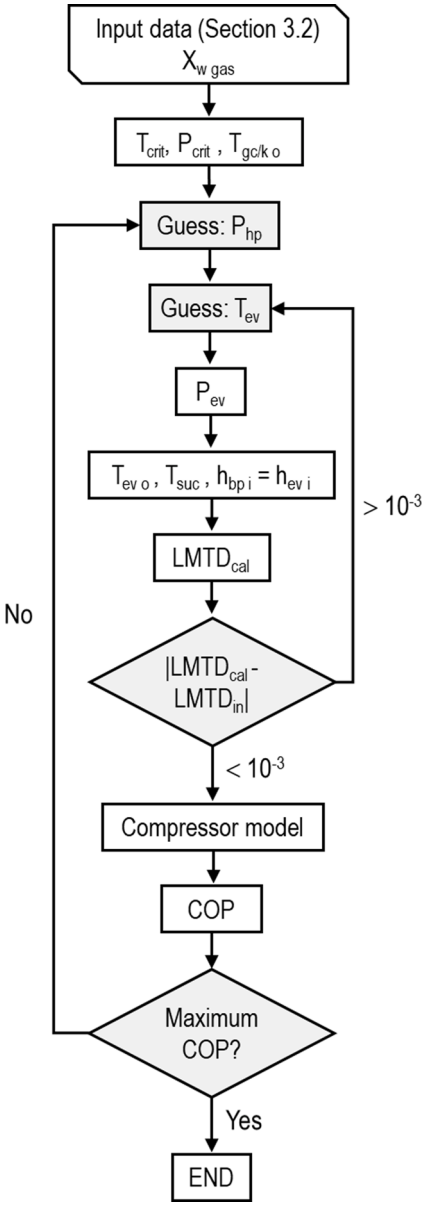

Fig. 5. Computational model flowchart.

3.3. Mathematical model

Fig. 5 describes the flowchart calculation of the mathematical model based on the principles of mass and energy conservation applied to the refrigeration components depicted in Fig. 4. MatLab® R2016a 64bits (https://es.mathworks.com/products/matlab.html) was used to execute the model with RefProp® v.10.0 (Lemmon et al., 2018) for the thermophysical properties calculation.

Taking the input data presented in Table 3, the developed model determines the maximum COP for each environmental temperature depending on the considered binary mixture. For this purpose, the model stars with a gas mass fraction (X_w gas) varied from 0% to a maximum of 20%, considering the limits presented in Table 2, determining the critical temperature and pressure of the mixture (T_{crit} and P_{crit}). It allows fixing the boundaries of subcritical and supercritical operation according to the environmental temperature (T_{env}). These limits determine the minimum and the maximum heat rejection pressure for the optimum calculation. Similar to (Catalán-Gil et al., 2018), Table 5 summarizes the ranges for P_{hp} according to the temperature at the exit of the gas-cooler / condenser ($T_{gc/k\ o}$) determined with Eq. (5) using the approach temperature (ΔT_{env}).

$$T_{gc/k\ o} = T_{env} + \Delta T_{env} \quad (5)$$

The condensing pressure (P_k) is calculated at liquid-saturated conditions. If $T_{env} < T_{crit}$ and $T_{gc/k\ o} < T_{crit}$, the subcritical and supercritical regime is possible. Therefore, the regime selected will be the one that maximises the COP of the plant.

Once the range is determined, the model varies P_{hp} with an increment of 0.1 bar until the optimal heat rejection pressure is determined. Similar to this iterative loop, the model includes a nested second loop to find the evaporating temperature (T_{ev}) using the logarithmic mean temperature difference (LMTD). This loop depends on the enthalpy at the evaporator inlet ($h_{ev\ i}$), which is equal to the enthalpy at the back-pressure inlet ($h_{bp\ i}$) assuming an isenthalpic expansion process. Further, if there is no heat transfer with surroundings from the exit of the gas-cooler/condenser to the inner of the back-pressure, $h_{bp\ i}$ is equal to the enthalpy at the gas-cooler/condenser outlet ($h_{gc/k\ o}$) (Eq. 6)

$$h_{bp\ i} = h_{ev\ i} = h_{gc/k\ o} \quad (6)$$

Neglecting the useful superheating (SH_{ev}), the logarithmic mean temperature difference in the evaporator ($LMTD_{cal}$) is calculated with Eq. (7), taking into account the non-azeotropic conditions of the mixture. $T_{ev\ i}$ is determined with the enthalpy hev i and the evaporating pressure (P_{ev}) at saturated-vapour conditions.

$$LMTD_{cal} = \frac{(T_{air\ i} - T_{ev\ o}) - (T_{air\ o} - T_{ev\ i})}{\ln\left(\frac{T_{air\ i} - T_{ev\ o}}{T_{air\ o} - T_{ev\ i}}\right)} \quad (7)$$

The result from Eq. 7 is compared to the input data in Table 3 for an iterative process that allows determining the evaporating temperature and also, the evaporating pressure.

Concerning the compressor model, the volumetric and the global efficiencies (η_G, η_V) are calculated with Eq. (3) and Eq. (4) and Table 4. The compressor power consumption ($\dot{W}$), the refrigerant mass flow rate ($\dot{m}$) and the suction temperature (T_{suc}) are defined through Eq. (8), Eq. (9) and Eq. (10), respectively.

Table 5
Heat rejection pressure limits depending on the environmental temperature.

Criterion	$T_{gc/k\ o}$		Regime	$P_{hp\ min}$	$P_{hp\ max}$
$T_{env} < T_{crit}$	$T_{env} + 5$	$T_{gc/k\ o} < T_{crit}$	SUBCRITICAL or SUPERCRITICAL	P_k or P_{crit}	120 bar
		$T_{gc/k\ o} > T_{crit}$	SUPERCRITICAL	P_{crit}	120 bar
$T_{env} > T_{crit}$	$T_{env} + 2$	$T_{gc/k\ o} > T_{crit}$	SUPERCRITICAL	P_{crit}	120 bar

$$\dot{W} = \dot{m}\frac{(h_{dis\ iso} - h_{suc})}{\eta_G} \tag{8}$$

$$\dot{m} = \frac{\dot{Q}_{ev}}{(h_{ev\ o} - h_{ev\ i})} \tag{9}$$

$$T_{suc} = T_{ev\ o} + SH_{suc} \tag{10}$$

Finally, the COP of the refrigerating cycle and the cubic capacity of the compressor ($\dot{V}_G$) are obtained by Eq. (11) and Eq. (12), respectively.

$$COP = \frac{\dot{Q}_{ev}}{\dot{W}} \tag{11}$$

$$\dot{V}_G = \frac{\dot{m} v_{suc}}{\eta_V} \tag{12}$$

Once the COP is obtained, the model starts with a new heat rejection pressure until the maximum COP is determined. This sequence is repeated for different mass fractions of CO_2 with increments of 2%, resulting in a 3D matrix where COP, environmental temperature and CO_2 mass fraction are related.

Finally, to compare pure-CO_2 with CO_2-doped blends, the variables of COP, optimum heat rejection pressure and cubic compressor capacity were considered to analyse the effect on the energy efficiency of the plant, the optimum operating conditions and the size of the compressor needed, respectively. Thus, equations Eq. (13), Eq. (14) and Eq. (15) are used to determine the variations of COP (ΔCOP), optimal heat rejection pressure ($\Delta P_{hp\ opt}$), and cubic compressor capacity ($\Delta\dot{V}_G$), respectively.

$$\Delta COP = \frac{COP_{blend} - COP_{CO2}}{COP_{CO2}} \tag{13}$$

$$\Delta P_{hp\ otp} = P_{hp\ otp\ blend} - P_{hp\ otp\ CO2} \tag{14}$$

$$\Delta\dot{V}_G = \frac{\dot{V}_{Cblend} - \dot{V}_{GCO2G}}{\dot{V}_{GCO2}} \tag{15}$$

The results from Eq. (13), Eq. (14) and Eq. (15) are discussed in Section 4, presenting the results as contour maps to highlight the variations of mixtures regarding pure-CO_2.

4. Results and discussion

This section discusses the results obtained using pure CO_2 and its corresponding binary blends. At first, pure CO_2 is analysed to determine the reference conditions. Later, CO_2-doped mixtures defined in Table 2 are evaluated at the same operating conditions but varying the mass fraction of the dopant fluid.

4.1. Pure C_{O2}

Fig. 6 shows the results obtained with COP, optimum heat rejection pressure ($P_{hp\ opt}$) and compressor cubic capacity ($\dot{V}_G$), depending on the environmental temperature.

The results demonstrate that COP drops as the environmental temperature rises (Fig. 6A), with an intermediate transition from subcritical to supercritical regime depending on boundary conditions described in Table 5. However, the effect on the optimal heat rejection pressure is just the opposite since the pressure rises as the temperature rises (Fig. 6B). It should be noticed that the optimal pressure has two constant regions: first, due to the restriction of the compression ratio at low environmental temperatures, and another at the transition zone from 22°C to 28°C. Concerning this, current back-pressure controllers establish a smooth pressure variation from the subcritical to the supercritical regime to avoid abrupt changes in pressure (Catalán-Gil et al., 2018). However, this method does not guarantee the maximum COP of the plant, so this work does not consider this smooth change.

Finally, the impact of the environmental temperature on the compressor cubic capacity (Fig. 6C) reveals the need to increase it as the temperature is higher to maintain the same cooling capacity. That means the use of different compressors in a compressor rack or the installation of a variable-speed compressor to overcome the effect of the environmental temperature. Regarding this last, the selected compressor has a frequency range from 30 to 70 Hz, which means a capacity range variation of ± 40% (Dorin, 2022). This information will be used in Section 4.2 to limit the doping gas mass fraction in the CO_2-based blends.

4.2. C_{O2}-doped blends

Sections 4.2.1 to 4.2.5 present and discuss the parameter increments calculated with equations Eq. (13), Eq. (14) and Eq. (15). To make clear

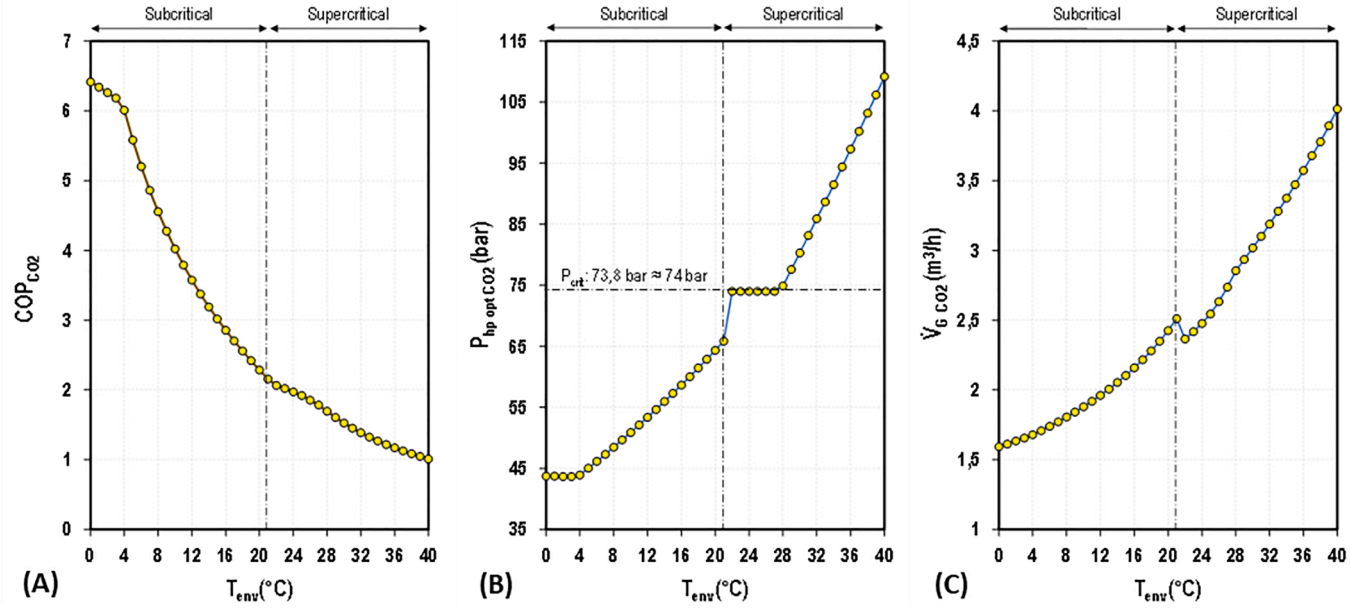

Fig. 6. COP (A), optimal heat rejection pressure (B) and compressor cubic capacity (C) for pure C_{O2}.

the visualisation, increments are presented as contour maps, where the environmental temperature is plotted on the X-axis, the flammable gas mass fraction on the Y-axis, and the analysed parameter as a colour contour line. The mass fraction is limited to 20% for R32, R152a, R1234yf and R1234ze(E) and 10% for the hydrocarbon R1270. These limits are lower than the results provided in Table 2 due to practical operating reasons since higher percentages of mass result in excessive compressor capacity increments.

Since the computational model search for optimal COP, the transient zone from subcritical to supercritical is different for each analysed fluid. This difference causes a disruption change in the studied parameters when comparing it with pure-CO_2 using equations Eq. (13) to Eq. (15). Therefore, the reader must be awarded that these variations are not applicable in a real operation of the refrigerating plant.

4.2.1. CO_2 / R32 mixture

Fig. 7 presents the variations of COP, optimal pressure and compressor cubic capacity for the binary blend of CO_2 and the HFC R32. According to Fig. 7A, the COP increases in almost all environmental temperatures except from 3 to 10°C. In this range, the impact is minimal or even harmful, with reductions up to -8.2% compared to pure CO_2. The best increments of COP are obtained at high environmental temperatures, with a maximum increment of +22.3% at the environmental temperature of 36°C and an R32 mass fraction of 20%. These results follow those obtained by Sun et al. (Sun et al., 2019), which reached increments of +31.2% with a heat rejection temperature of 45°C but using an R32 mass fraction of 40%.

Regarding the optimal heat rejection temperature (Fig. 7B), R32 reduces the optimal heat rejection pressure as the R32 mass fraction increases with a maximum reduction of -25.7 bar at 40°C and a gradual decrease at lower environmental temperatures. Dai et al. (Dai et al., 2015) first theoretically, and Sun et al. (Sun et al., 2019) and Sánchez et al. (Sánchez et al., 2023) later experimentally, demonstrate this working pressure reduction depending on the mass fraction charge of R32.

Finally, using of the CO_2/R32 blend increases the compressor cubic capacity to provide the same cooling capacity due to the reduction of the VCC stated in Fig. 3A (Fig. 7C). Assuming a maximum capacity variation of +40% over the nominal compressor capacity, the recommended fraction of R32 will be around 10% for a direct drop-in and up to 19% in a new plant design.

4.2.2. CO_2 / R152a mixture

The mixture of CO_2/R152a is treated in Fig. 8, resulting in an enhanced of COP at environmental temperatures above 30°C. The maximum increment reached is +12.2% at 40°C with an R152a mass fraction of 18%. Below this, adding R152a results in a negative impact with a sharp decrease at temperatures below 15°C. Dai et al. (Dai et al., 2015) verified the same effect using a heat rejection temperature of 15°C, while Xie et al. (Xie et al., 2021) observed COP increments with gas-cooler outlet temperature of 35°C with an R152a mass fraction of 12.5%. In both cases, the optimal heat rejection pressure presented a significant decrease due to the low density of R152a. This behaviour is depicted in Fig. 8B with higher reductions at high ambient temperatures excepting the transition zone from supercritical to subcritical.

Finally, using the binary mixture of CO_2/R152a results in a significant increment of the required compressor capacity (Fig. 8C) due to the reduced volumetric cubic capacity shown in Fig. 3A (the highest compared with other fluids). This aspect is vitally important in a drop-in process, where the recommended fraction of R152a will be around 4% for a maximum variation capacity of +40% through a frequency driver.

4.2.3. CO_2 / R1234yf mixture

The HFO R1234yf mixed with CO_2 positively enhances COP at environmental temperatures above 29°C, depending on the mass fraction (Fig. 9A). Below this, the effect of adding R1234yf results negative for the COP, excepting the transient zone from subcritical to supercritical and the region with low environmental temperatures. From the results, the maximum ΔCOP reached is +10.9% at 38°C with an R1234yf mass fraction of 20%. Notwithstanding, Vaccaro et al. (Vaccaro et al., 2022) computed an improvement of +12.8% at a heat rejection temperature of 40°C and an R1234yf mass fraction of 15%. However, the base cycle used in their study includes an IHX, which positively affects the COP (Torrella et al., 2011).

Focusing on optimal pressure (Fig. 9B), the R1234yf reduces the working pressures, excluding the transient zone from subcritical to supercritical. In any case, the maximum reduction is -24.7 bar at 40°C.

Lastly, the CO_2/R1234yf binary mixture requires higher compressor capacity than CO_2 (Fig. 9C) but significative lower than R152a due to the higher density of R1234yf. Considering a drop-in process, the recommended fraction of R1234yf will be around 6 - 8% considering the capacity variation of +40%.

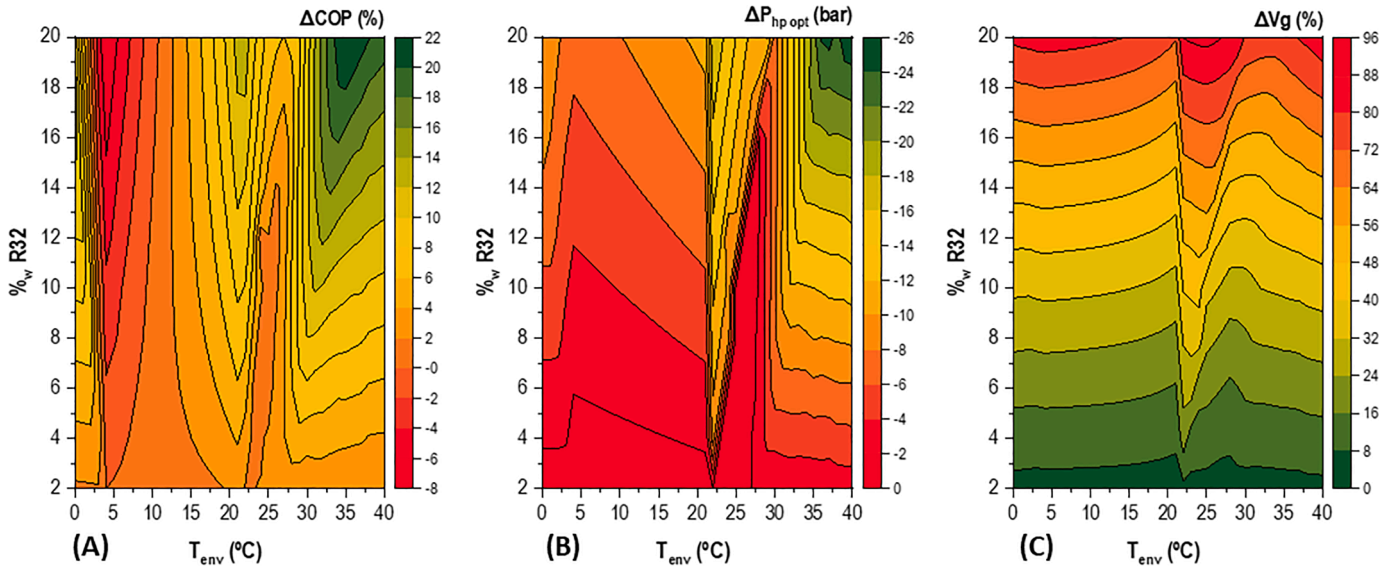

Fig. 7. ΔCOP (A), $\Delta P_{hp\ opt}$ (B) and $\Delta \dot{V}_G$ (C) for the CO_2 / R32 mixture.

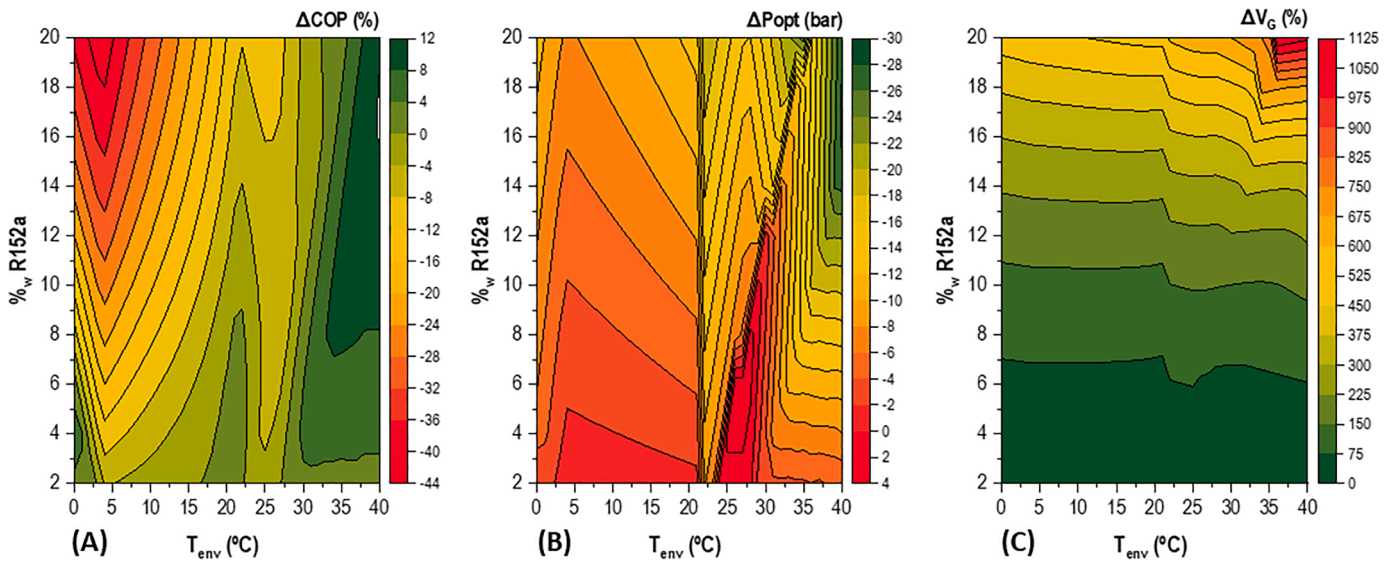

Fig. 8. ΔCOP (A), $\Delta P_{hp\ opt}$ (B) and $\Delta \dot{V}_G$ (C), for the CO_2 / R152a mixture.

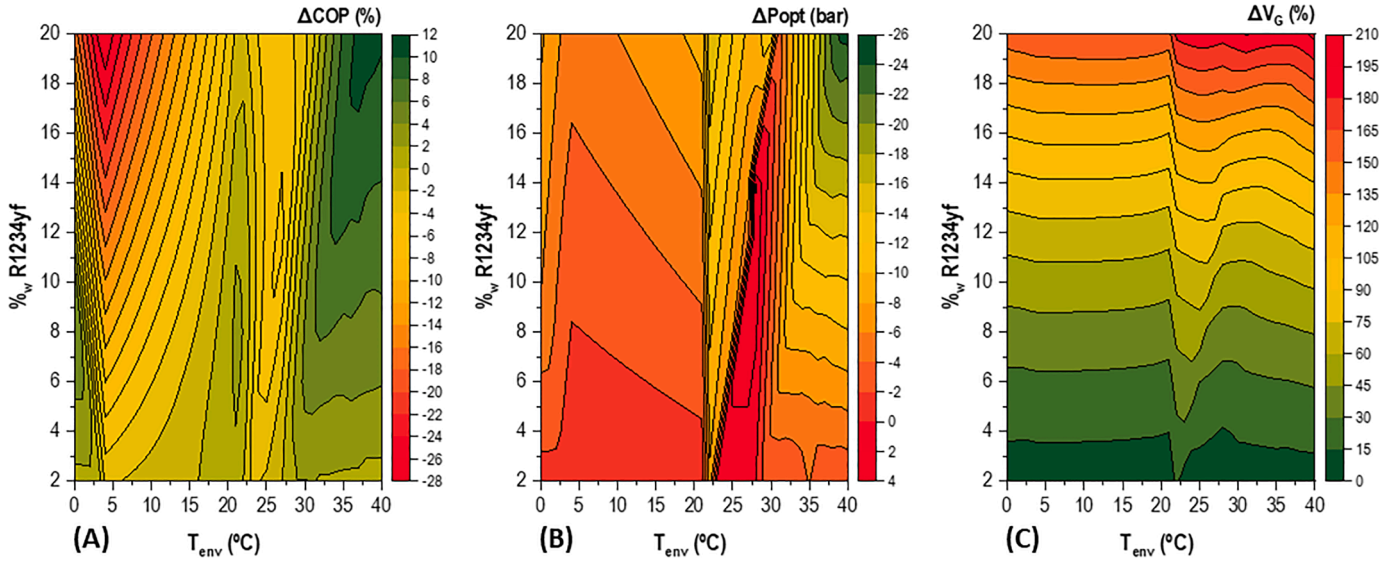

Fig. 9. ΔCOP (A), $\Delta P_{hp\ opt}$ (B) and $\Delta \dot{V}_G$ (C), for the CO_2 / R1234yf mixture.

4.2.4. CO_2 / R1234ze(E) mixture

For the HFO R1234ze(E), benefits in COP are only possible for environmental temperatures above 30°C with increments up to +7.3% at 40°C and a mass fraction of 20% (Fig. 10C). Below 30°C decrements are remarkable and negatively affect the refrigerating plant's COP, excepting the region with low environmental temperatures due to the limitation of the compression ratio. Despite this, the reduction in the optimum pressure reaches up to -27.8 bar at 40°C and a mass fraction of 20% (Fig. 10B).

Focusing on the cubic compressor capacity (Fig. 10C), the CO_2/R1234ze(E) blend requires a higher capacity than R1234yf. Therefore, If a drop-in process is carried out in an existing plant, the recommended mass fraction of R1234ze(E) will be around 4% attending to the maximum variation capacity stated before.

4.2.5. CO_2 / R1270 mixture

As alternative to R290, the hydrocarbon R1270 provides a full-natural blend that benefits COP in all temperature ranges, except those from 3 to 12°C and 23 to 28°C (Fig. 11A). Since the mass fraction of R1270 is limited to 7.6% due to the non-flammability conditions (Table 2), the maximum increment of COP is limited to +9.2% at 32°C. These results are followed by Sánchez et al. (Sánchez et al., 2023), which obtained energy savings of 4.3% at 30°C using a mixture of CO_2/R1270 (92.5/7.5% in mass).

Concerning the effect on the optimal heat rejection pressure (Fig. 11B), R1270 introduces a maximum reduction up to -12.2 bar at the mass fraction of 7.6%. Only in the transient zone from subcritical to supercritical the optimal pressure reports a maximum increment of about +2.5 bar due to the initial model assumptions.

According to Fig. 11C, the mixture of CO_2/R1270 requires a higher cubic capacity than pure CO_2. However, in a drop-in process, the mixture can be easily handled by the same CO_2 compressor using a frequency driver due to the limitation of the R1270 mass fraction.

4.3. Optimal mixture selection

The results presented in Section 4.2 confirm that there is no unique mixture solution to enhance the COP of the refrigerating plant.

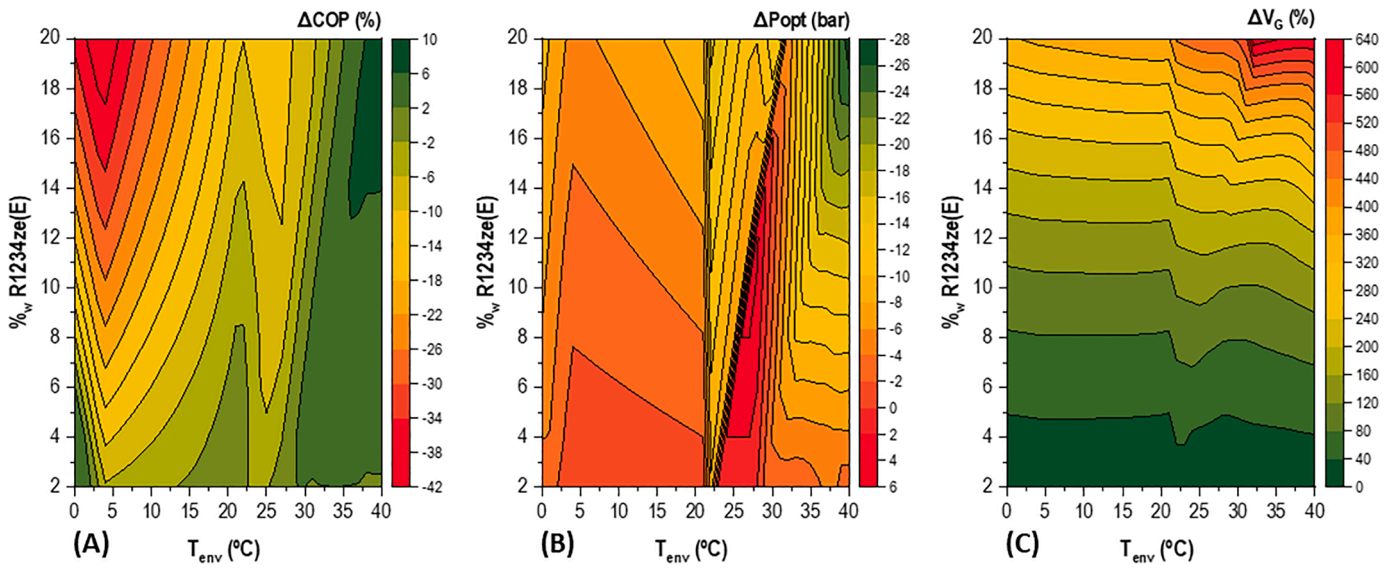

Fig. 10. ΔCOP (A), $\Delta P_{hp\ opt}$ (B) and $\Delta \dot{V}_G$ (C), for the CO_2 / R1234ze(E) mixture.

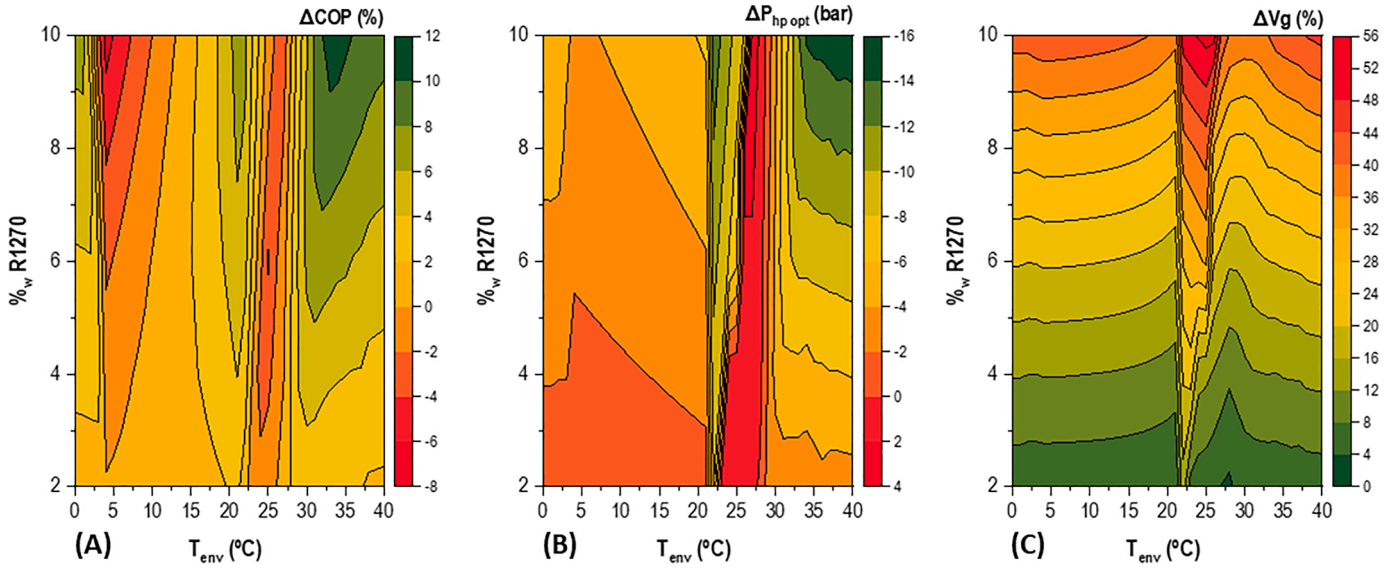

Fig. 11. ΔCOP (A), $\Delta P_{hp\ opt}$ (B) and $\Delta \dot{V}_G$ (C), for the CO_2 / R1270 mixture.

Table 6
Binary mixtures composition and results attending a new plant design or a drop-in in an existing plant.

Mixture	Temperature range (°C)	Existing plant (*drop-in*) Gas mass fraction	ΔCOP_{avg}	$\Delta \dot{V}_{G\ avg}$	$\Delta P_{hp\ opt\ avg}$	New design Gas mass fraction	ΔCOP_{avg}	$\Delta \dot{V}_{G\ avg}$	$\Delta P_{hp\ opt\ avg}$
CO_2 / R32	0 - 12 °C	10%	1.76%	33.55%	-4.32 bar	19%	0.18%	76.84%	-7.75 bar
	13 - 26 °C		4.50%	33.82%	-5.75 bar		7.73%	76.43%	-11.13 bar
	27 - 40 °C		9.81%	32.34%	-9.77 bar		15.78%	75.47%	-16.61 bar
CO_2 / R152a	0 - 12 °C	4%	-4.03%	35.40%	-2.58 bar	6%	-8.38%	60.43%	-3.57 bar
	13 - 26 °C		-1.37%	37.64%	-3.04 bar		-2.63%	64.07%	-4.72 bar
	27 - 40 °C		4.14%	37.44%	-5.29 bar		4.77%	65.27%	-7.03 bar
CO_2 / R1234yf	0 - 12 °C	7%	-3.49%	33.01%	-2.58 bar	12%	-9.27%	68.68%	-4.11 bar
	13 - 26 °C		-1.27%	35.66%	-3.45 bar		-2.72%	73.24%	-6.28 bar
	27 - 40 °C		3.90%	34.64%	-5.58 bar		4.54%	74.93%	-8.70 bar
CO_2 / R1234ze(E)	0 - 12 °C	4%	-4.74%	31.79%	-1.97 bar	6%	-8.75%	52.63%	-2.71 bar
	13 - 26 °C		-2.59%	33.80%	-1.81 bar		-4.23%	56.32%	-2.98 bar
	27 - 40 °C		2.53%	34.43%	-3.98 bar		2.75%	58.06%	-5.40 bar
CO_2 / R1270	0 - 12 °C	7.5%	0.38%	27.73%	-3.46 bar	7.5%	0.38%	27.73%	-3.46 bar
	13 - 26 °C		2.16%	29.50%	-5.25 bar		2.16%	29.50%	-5.25 bar
	27 - 40 °C		6.14%	29.63%	-7.59 bar		6.14%	29.63%	-7.59 bar

Therefore, for each binary mixture, the desirable CO_2 mass fraction will attempt the criterion to maintain the highest COP increment in all tested environmental temperatures. However, there is a limitation of volumetric compressor capacity that can be addressed from two points of view:

a) Existing plants. Assuming full compatibility with oil, the binary mixture can be added to an existing plant by a drop-in, modifying the control of the expansion valves and the cubic capacity of the compressor by adding a frequency driver. Considering that the rotation speed range of a semihermetic compressor goes from 30 to 70 Hz (Dorin, 2022), the maximum increment possible is +40%.
b) New design. In a new refrigerating plant design, the compressor capacity can easily select. In this case, the maximum cubic capacity assumed is +140%.

Considering the limitation stated above, Table 6 summarizes the limits of binary mixtures in the environmental temperature range from 0 to 40°C. The results in COP, compressor cubic capacity and optimal pressure, are averaged in three temperature ranges depending on the environmental conditions: low (0 to 12°C), warm (13 to 26°C) and high (27 to 40°C).

The results in Table 6 of the selected binary mixture compositions are depicted in Figs. 12 and 13, including the optimal heat rejection pressure. These results showed that all binary mixtures improve the COP at high environmental temperatures. For example, CO_2/R32 and CO_2/R1270 provide the best results in new designs with increments up to +15.78% and +6.14%, respectively, while in a drop-in process, the results are +9.81% and +6.14%, respectively. Moreover, both mixtures increase the COP in all temperature ranges, which makes these mixtures very attractive for different environmental temperatures.

For blends of CO_2/R152a, CO_2/R1234yf and CO_2/R1234ze(E), the benefits of COP are only positive at the range of high temperature with values from 2.53% to 4.14%. However, it is important to highlight that the transition zone from subcritical to supercritical has not been optimized in the computational model, so the workability of mixtures may be higher than the proposed ranges.

Regarding the optimal heat rejection pressure, mixtures reduce this value compared with pure CO_2 except in the transition zone. However, as mentioned above, this zone has not been optimized, so a reduction in the environmental temperature range is expected, which benefits component design, compressor operation and pressure range operation. According to Fig. 12, new optimal pressure correlations should be developed for these mixtures considering the smooth transition from subcritical to supercritical.

5. Conclusions

This work analyses five CO_2-based binary mixtures using R32, R152a, R1234yf, R1234ze(E) and R1270 as doping fluids to enhance the performance of a transcritical refrigeration plant. Maintaining the conditions of non-flammability and GWP below 150, the CO_2-doped blends allow increasing the critical temperature above 31°C providing the opportunity to operate in subcritical conditions at high environmental temperatures. Consequently, the cycle operating pressures decrease, easing the operation and the control of the refrigerating plant, including the optimal heat rejection pressure. However, despite the positive effect in pressure terms, the studied mixtures result in lower values of volumetric cubic capacity which entails larger compressor sizes for the desired cooling capacity.

Considering a medium-temperature application for fresh-food preservation, a computational model has been developed to evaluate the five CO_2-based binary mixtures in a wide range of environmental temperatures from 0 to 40°C. The results obtained evidence that the maximum COP increments are obtained at high temperatures, with maximum increments of +22.3% adding an R32 mass fraction of 20% R32, +12.2% using an R152a mass fraction of 18%, +10.9% with an R1234yf mass fraction of 20%, +7.3% with an R1234ze(E) mass fraction of 20%, and

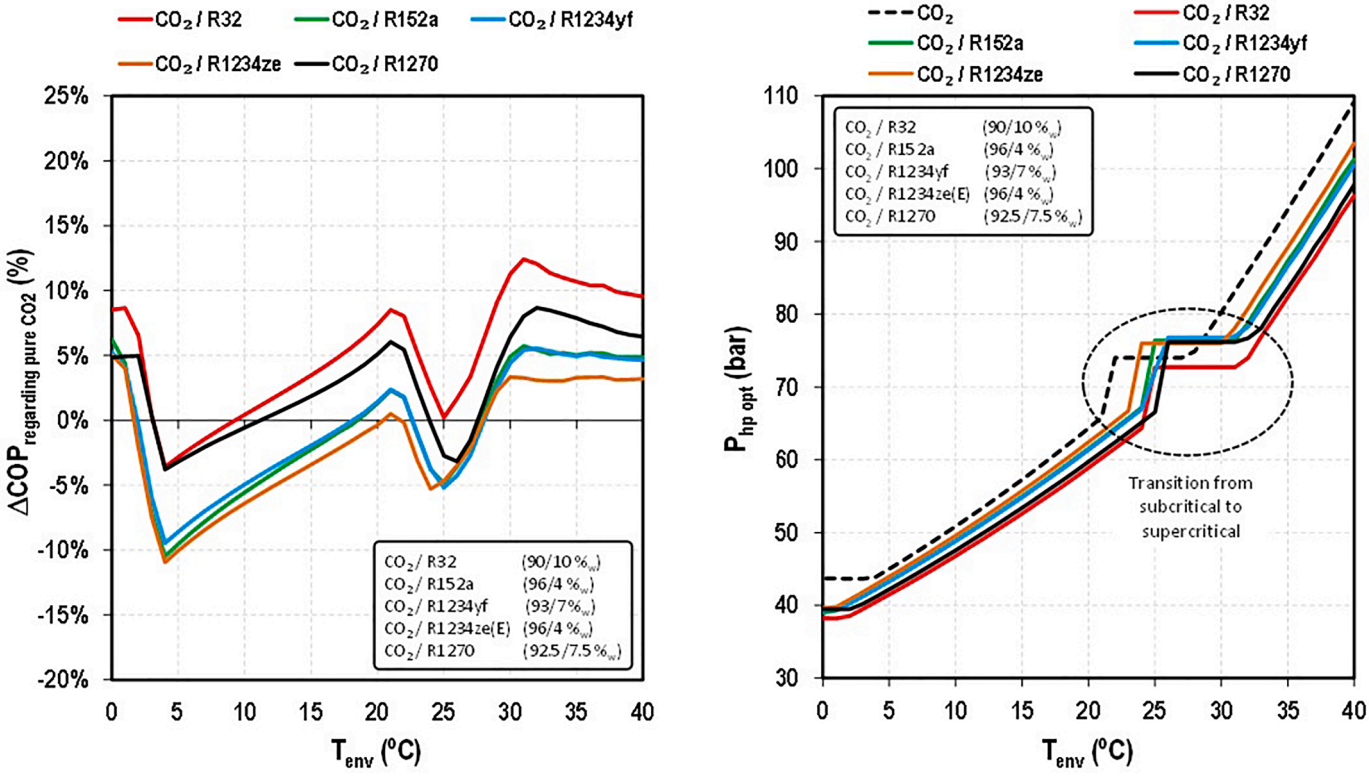

Fig. 12. Variation of ΔCOP and optimal heat rejection pressure ($P_{hp\ opt}$) in a drop-in process (existing plant).

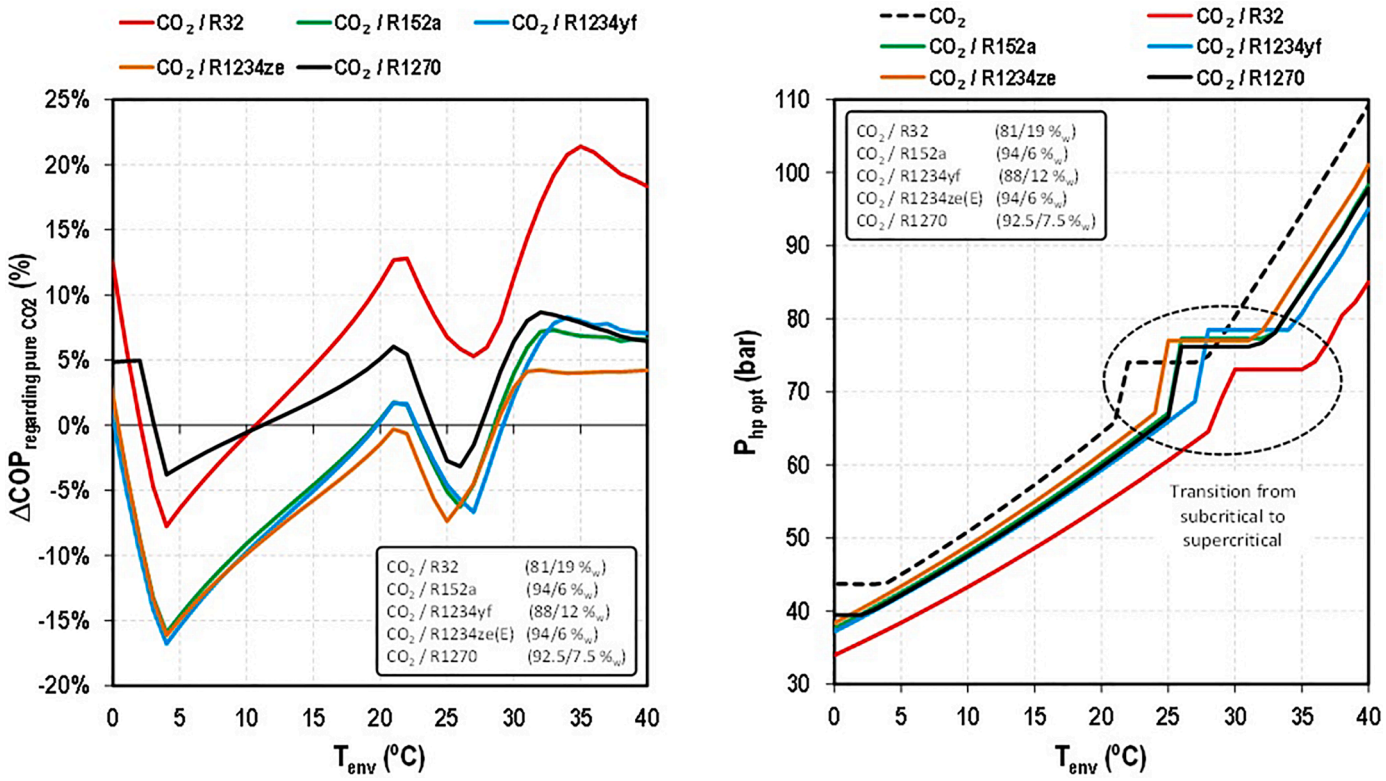

Fig. 13. Variation of ΔCOP and optimal heat rejection pressure ($P_{hp\ opt}$) in a new plant design.

+9.2% with an R1270 mass fraction of 7.6%. Furthermore, these mixtures reduce the optimum heat rejection pressure up to 29 bar reducing the compressor discharge pressure. However, the selected mass fractions report important reductions in the volumetric cubic capacity, affecting the compressor size and the cost of the refrigerating plant.

Considering this issue, two cases have been proposed to optimize the binary mixtures' mass fraction, attempting the compressor volumetric cubic capacity. Thus, for existing plants where a drop-in process is applied, and the compressor cubic capacity can be modified only by a frequency driver, the best-recommended mixtures are CO_2/R32 (90/10%w) and CO_2/R1270 (92.5/7.5%w). The maximum increments of COP reached by both mixtures are +12.41% and +8.66%, respectively, with average values in the tested environmental temperature of +5.36% and +2.90%, respectively. In new refrigerating plants where the compressor size is not fixed previously, the best-recommended mixtures are CO_2/R32 (81/19%w) and CO_2/R1270 (92.5/7.5%w), with maximum increments of COP of +21.39% and +8.66%, respectively. The average values in the tested environmental temperature are +7.89% and +2.90%, respectively.

In summary, using CO_2-based blends demonstrates the possibility of efficiently improving CO_2 transcritical cycles' performance without including complex arrangements exclusively used in high-capacity systems. However, additional experimental tests are necessary to verify the above results, including heat transfer processes, compressor operation and optimal pressure regulation.

Declaration of Competing Interest

The authors declare that they have no known competing financial interests or personal relationships that could have appeared to influence the work reported in this paper.

Acknowledgements

This article is part of the project PID2021–126926OB-C21 (acronym: HELTHA), funded by the Spanish Ministry of Science and Innovation. The authors would like to acknowledge the economic support to this study by the European Union – "NextGenerationEU" through the grant INVEST/2022/294 to R. Larrondo, the Ministry of Science, Innovation and Universities for the research grant PRE2019–091617 to F. Vidan, the European Union - NextGenerationEU "NextGenerationEU"/PRTR for the research project TED2021-130162B-I00, and the Jaume I University for the research project UJI-B2021–10.

References

Aranguren, P., Sánchez, D., Casi, A., Cabello, R., Llopis, R., Astrain, D., 2021. Experimental assessment of a thermoelectric subcooler included in a transcritical CO_2 refrigeration plant. Appl. Therm. Eng. 190, 116826 https://doi.org/10.1016/j.applthermaleng.2021.116826.

ASHRAE, Standard 34–2019. Designation and safety classification of refrigerants (2019).

Bell, I.H., Lemmon, E.W., 2016. Automatic fitting of binary interaction parameters for multi-fluid Helmholtz-energy-explicit mixture models. J. Chem. Eng. Data 61, 3752–3760. https://pubs.acs.org/doi/pdf/10.1021/acs.jced.6b00257.

Bell, I.H., Riccardi, D., Bazyleva, A., McLinden, M.O., 2021. Survey of data and models for refrigerant mixtures containing halogenated olefins. J. Chem. Eng. Data 66, 2335–2354. https://pubs.acs.org/doi/pdf/10.1021/acs.jced.1c00192.

Bellos, E., Tzivanidis, C., 2019. Enhancing the performance of a C_{O2}refrigeration system with the use of an absorption chiller. Int. J. Refrig. 108, 37–52. https://doi.org/10.1016/j.ijrefrig.2019.09.009.

Bouteiller, P., Terrier, M.F., Tobaly, P., 2016. A methodology and bench design for experimental study of heat pump thermodynamic cycles using C_{O2}based mixtures. 12th IIR- Gustav Lorentzen Nat. Working Fluids Conference, Edinburgh 1015. https://doi.org/10.18462/iir.gl.2016.1015. Paper.

Bouteiller, P., Terrier, M.F., Tobaly, P., 2017. Experimental study of heat pump thermodynamic cycles using CO_2 based mixtures - methodology and first results. AIP Conference Proceed. 1814, 020052 https://doi.org/10.1063/1.4976271.

Cabello, R., Sánchez, D., Patiño, J., Llopis, R., Torrella, E., 2012. Experimental analysis of energy performance of modified single-stage CO_2transcritical vapour compression cycles based on vapour injection in the suction line. Appl. Therm. Eng. 47 (5), 86–94. https://doi.org/10.1016/j.applthermaleng.2012.02.031.

Calm, J.M., 1999. ARTI refrigerant database. Data summaries - Volume 1: single-compound refrigerants. Air-Conditioning and Refrig. Technol. Institute. Reference. DOE/CE/23810-105.

Catalán-Gil, J., Sánchez, D., Cabello, R., Llopis, R., Nebot-Andrés, L., Calleja-Anta, D., 2020. Experimental evaluation of the desuperheater influence in a CO_2booster refrigeration facility. Appl. Therm. Eng. 168 (5), 114785 https://doi.org/10.1016/j.applthermaleng.2019.114785.

Catalán-Gil, J., Sánchez, D., Llopis, R., Nebot-Andrés, L., Cabello, R., 2018. Energy evaluation of multiple stage commercial refrigeration architectures adapted to F-Gas regulation. Energies 11 (7), 1915. https://doi.org/10.3390/en11071915.

Chesi, A., Esposito, F., Ferrara, G., Ferrari, L., 2014. Experimental analysis of R744 parallel compression cycle. Appl. Energy 135 (15), 274–285. https://doi.org/10.1016/j.apenergy.2014.08.087.

IPCC. Climate Change 2014: Synthesis Report. Contribution of Working Groups I, II and III to the Fifth Assessment Report of the Intergovernmental Panel On Climate Change [Core Writing Team, R.K. Pachauri and L.A. Meyer (eds.)]. IPCC, Geneva, Switzerland (2014).

Cox, N., Mazur, V., Colbourne, D., 2008. New high pressure low-GWP azeotropic and near-azeotropic refrigerant blends. In: International Refrigeration and Air Conditioning Conference. Paper 987. http://docs.lib.purdue.edu/iracc/987.

Dai, B., Dang, C., Li, M., Tian, H., Ma, Y., 2015. Thermodynamic performance assessment of carbon dioxide blends with low-global warming potential (GWP) working fluids for a heat pump water heater. Int. J. Refrig. 56, 1–14. https://doi.org/10.1016/j.ijrefrig.2014.11.009.

Dorin. CD SERIES semi-hermetic motor compressors transcritical CO_2 application –50/60Hz (2022). Available on: https://www.dorin.com/documents/Download/18/1LTZ016_CD_02.22_rev.pdf.

Di Nicola, G., Giuliani, G., Polonara, F., Stryjek, R., 2005. Blends of carbon dioxide and HFCs as working fluids for the low-temperature circuit in cascade refrigerating systems. Int. J. Refrig. 28, 130–140. https://doi.org/10.1016/j.ijrefrig.2004.06.014.

Elbel, S., Hrnjak, P., 2004. Flash gas bypass for improving the performance of transcritical R744 systems that use microchannel evaporators. Int. J. Refrig. 27 (7), 724–735. https://doi.org/10.1016/j.ijrefrig.2004.07.019.

Haida, M., Banasiak, K., Smolka, J., Hafner, A., Eikevik, T.M., 2016. Experimental analysis of the R744 vapour compression rack equipped with the multi-ejector expansion work recovery module. Int. J. Refrig. 64, 93–107. https://doi.org/10.1016/j.ijrefrig.2016.01.017.

Hodnebrog, Ø., Dalsøren, S.B., Myhre, G., 2018. Lifetimes, direct and indirect radiative forcing, and global warming potentials of ethane (C2H6), propane (C3H8), and butane (C4H10). Atmospheric Sci. Lett. 19 (2), e804. https://doi.org/10.1002/asl.804.

Honeywell, 2008. HFO-1234yf low GWP refrigerant update. Int. Refrig. Air Conditioning Conference on. Presentation. Available. https://www.honeywell-refrigerants.com/india/?document=2008-purdue-conference-low-gwp-refrigerants&download=1.

Honeywell, 2018. Technical brochure.

IPCC, 2021. Climate Change 2021: The Physical Science Basis. Contribution of Working Group I to the Sixth Assessment Report of the Intergovernmental Panel On Climate Change [Masson-Delmotte. Cambridge University Press, Cambridge, United Kingdom and New York, NY, USA, pp. 2391–pp. https://doi:10.1017/9781009157896.

Ju, F., Fan, X., Chen, Y., Ouyang, H., Kuang, A., Ma, S., Wang, F., 2018. Experiment and simulation study on performances of heat pump water heater using blend of R744/R290. Energy & Build. 169, 148–156. https://doi.org/10.1016/j.enbuild.2018.03.063.

Kim, J.H., Cho, J.M., Kim, M.S., 2008. Cooling performance of several C_{O2}/propane mixtures and glide matching with secondary heat transfer fluid. Int. J. Refrig. 31 (5), 800–806. https://doi.org/10.1016/j.ijrefrig.2007.11.009.

Kim, M.H., Pettersen, J., Bullard, C.W., 2004. Fundamental process and system design issues in C_{O2}vapor compression systems. Progress in Energy and Combustion Sci. 30 (2), 119–174. https://doi.org/10.1016/j.pecs.2003.09.002.

Kim, S.G., Kim, M.S., 2002. Experiment and simulation on the performance of an autocascade refrigeration system using carbon dioxide as a refrigerant. Int. J. Refrig. 25, 1093–1101. https://doi.org/10.1016/S0140-7007(01)00110-4.

Kondo, S., Takizawa, K., Takahashi, A., Tokuhashi, K., 2006. Extended Le Chatelier's formula for carbon dioxide dilution effect on flammability limits. J. Hazardous Mater. A138, 1–8. https://doi.org/10.1016/j.jhazmat.2006.05.035.

Lemmon, E.W., Bell, I.H, Huber, M.L., McLinden, M.O, 2018. REFPROP Reference Fluid Thermodynamic and Transport Properties. NIST Standard Reference Database 23 10 (0). Version.

Lorentzen, G., 1995. The use of natural refrigerants: a complete solution to the CFC/HCFC predicament. Int. J. Refrig. 18 (3), 190–197. https://doi.org/10.1016/0140-7007(94)00001-E.

MathWorks. *MatLab R2016a 64 bits* (2016). Availabe on: https://es.mathworks.com/products/matlab.html.

Morlet, V., Coulomb, D., Dupond, J.L., 2017. The impact of the refrigeration sector on climate change. 35thinformatory note on refrigeration technologies. IIR [on line]. Available on https://iifiir.org/en/fridoc/the-impact-of-the-refrigeration-sector-on-climate-change-141135.

Mulroy, W.J., Domanski, P.A., Didion, D.A., 1994. Glide matching with binary and ternary zeotropic refrigerant mixtures Part 1. An experimental study. Int. J. Refrig. 17 (4), 220–225. https://doi.org/10.1016/0140-7007(94)90037-X.

Niu, B., Zhang, Y., 2007. Experimental study of the refrigeration cycle performance for the R744/R290 mixtures. Int. J. Refrig. 30 (1), 37–42. https://doi.org/10.1016/j.ijrefrig.2006.06.002.

Raabe, G., 2013. Molecular simulation studies on the vapor−liquid phase equilibria of binary mixtures of R1234yf and R1234ze(E) with R32 and CO_2. J. Chem. Eng. Data 58, 1867–1873. https://pubs.acs.org/doi/pdf/10.1021/je4002619?src=getftr.

Sánchez, D., Catalán-Gil, J., Cabello, R., Calleja-Anta, D., Llopis, R., Nebot-Andrés, L., 2020. Experimental analysis and optimization of an R744 Transcritical cycle working with a mechanical subcooling system. Energies 13 (12), 3204. https://doi.org/10.3390/en13123204.

Sánchez, D., Catalán-Gil, J., Llopis, R., Nebot-Andrés, L., Cabello, R., Torrella, E., 2018. CO_2 vs. Fluorinated refrigerants energy evaluation in a mt cabinet with DX-system. 13th IIR- Gustav Lorentzen on Nat. Refrig., Valencia 119. https://doi.org/10.18462/iir.gl.2018.1119. Paper.

Sánchez, D., Patiño, J., Llopis, R., Cabello, R, Torrella, E., Vicente Fuentes, F, 2014. New positions for an internal heat exchanger in a CO_2 supercritical refrigeration plant. Experimental analysis and energetic evaluation. Appl. Therm. Eng. 63 (1), 129–139. https://doi.org/10.1016/j.applthermaleng.2013.10.061.

Sánchez, D., Vidan-Falomir, F., Nebot-Andrés, L., Llopis, R., Cabello, R., 2023. Alternative blends of CO_2 for transcritical refrigeration systems. Experimental approach and energy analysis. Energy Conversion and Manag. 279, 116690 https://doi.org/10.1016/j.enconman.2023.116690.

Sarkar, J., Bhattacharyya, S., 2009. Assessment of blends of CO_2 with butane and isobutane as working fluids for heat pump applications. Int. Journal of Therm. Sci. 48, 1460–1465. https://doi.org/10.1016/j.ijthermalsci.2008.12.002.

Singh, S., Maiya, P.M., Hafner, A., Banasiak, K., Neksa, P., 2020. Energy efficient multiejector CO_2 cooling system for high ambient temperature. Therm. Sci. Eng. Progress 19 (1), 100590. https://doi.org/10.1016/j.tsep.2020.100590.

Sun, Z., Cui, Q., Wang, Q., Ning, J., Guo, J., Dai, B., Liu, Y., Xu, Y., 2019. Experimental study on CO_2/R32 blends in a water-to-water heat pump system. Appl. Therm. Eng. 162, 114303 https://doi.org/10.1016/j.applthermaleng.2019.114303.

Torrella, E., Sánchez, D., Llopis, R., Cabello, R., 2011. Energetic evaluation of an internal heat exchanger in a CO_2 transcritical refrigeration plant using experimental data. Int. J. Refrig. 34 (1), 40–49. https://doi.org/10.1016/j.ijrefrig.2010.07.006.

Vaccaro, G., Milazzo, A., Talluri, L., 2022. Thermodynamic assessment of trans-critical refrigeration systems utilizing CO_2-based mixtures. Int. J. Refrig. 147, 61-70. doi.org/10.1016/j.ijrefrig.2022.09.013.

Wang, D., Lu, Y., Tao, L., 2017. Thermodynamic analysis of CO_2 blends with R41 as an azeotropy refrigerant applied in small refrigerated cabinet and heat pump water heater. Appl. Therm. Eng. 125, 1490–1500. https://doi.org/10.1016/j.applthermaleng.2017.07.009.

Xie, J., Wang, J., Lyu, Y., Wang, D., Peng, X., Liu, H., Xiang, S., 2021. Numerical investigation on thermodynamic performance of CO2-based mixed refrigerants applied in transcritical system. J. Therm. Anal. Calorimetry 147, 6883–6892. https://doi.org/10.1007/s10973-021-11011-x.

Yu, B., Wang, D., Liu, C., Jiang, F., Shi, J., Chen, J., 2018. Performance improvements evaluation of an automobile air conditioning system using CO_2-propane mixture as a refrigerant. Int. J. Refrig. 88, 172–181. https://doi.org/10.1016/j.ijrefrig.2017.12.016.